General Disclaimer

One or more of the Following Statements may affect this Document

- This document has been reproduced from the best copy furnished by the organizational source. It is being released in the interest of making available as much information as possible.

- This document may contain data, which exceeds the sheet parameters. It was furnished in this condition by the organizational source and is the best copy available.

- This document may contain tone-on-tone or color graphs, charts and/or pictures, which have been reproduced in black and white.

- This document is paginated as submitted by the original source.

- Portions of this document are not fully legible due to the historical nature of some of the material. However, it is the best reproduction available from the original submission.

Quarterly Technical Report No. 3

Covering the Period 1 May 1972 through 31 July 1972

DEVELOPMENT OF GaAs SOLAR CELLS

Contract No. 953270

Submitted to:

Jet Propulsion Laboratory
California Institute of Technology
488 Oak Grove Drive
Pasadena, California 91103

(NASA-CR-129199) DEVELOPMENT OF GaAs SOLAR CELLS Quarterly Technical Report, 1 May - 31 Jul. 1972 (Ion Physics Corp.) 31 Jul. 1972 21 p CSCL 10A

N73-11042

Unclas
G3/03 47511

Approved by: _____

F.T.C. Bartels
Division Manager

This work was performed for the Jet Propulsion Laboratory, California Institute of Technology, sponsored by the National Aeronautics and Space Administration under Contract NAS7-100.

ION PHYSICS CORPORATION IPC

A Subsidiary of High Voltage Engineering Corporation

BURLINGTON, MASSACHUSETTS

TABLE OF CONTENTS

LIST OF ILLUSTRATIONS

LIST OF TABLES

1. SUMMARY

Solar cells and mesa diodes were fabricated by the implantation of zinc or beryllium ions into N-type gallium arsenide ($N_D \sim 2 \times 10^{17}$ cm^{-3}). Annealing temperatures above 750 °C (zinc) or 650 °C (beryllium) were found to produce 50% to 100% activation of the implanted ions, up to acceptor concentrations of approximately 2×10^{19} cm^{-3}. Junction depths of about 0.4 micron were produced by 600 keV zinc implants or 70 keV beryllium implants. P-layer sheet resistance was about 150 ohms for 2×10^{15} cm^{-2} zinc or 1×10^{15} cm^{-2} beryllium implants. This is sufficiently low for efficient solar cell fabrication. Contacting procedures were improved to yield reproducibly adherent, low resistance front and back contacts.

The devices were characterized by C-V, dark and illuminated I-V, and spectral response measurements. The C-V measurements show that the P^+N junction is nearly abrupt, and that no compensated layer exists at the junction. The dark I-V measurements show that junction characteristics are dominated by recombination centers in the junction space-charge region up to forward voltages of about 0.9 volt. At the theoretical photogenerated current density of 35 mA/cm^2, the forward voltage drop of the best diodes is 0.96 volt, which implies that the base region lifetime is about 10^{-9} seconds. This is close to the value in unprocessed material, indicating that the processing used does not greatly degrade the base lifetime. The illuminated I-V measurements show very low short-circuit current (about 5 mA/cm^2), and the spectral response measurements show that this current arises almost entirely from carriers generated in the base region; i.e., the surface region photoresponse is almost zero.

By etching device samples in a structure-sensitive etchant, we have determined that the surface preparation technique used to fabricate these devices was not effective in removing mechanical damage from the polishing operations. A new surface preparation technique was developed, and it appears to produce damage-free surfaces, and therefore should improve the surface region photoresponse. Other process changes which we expect will improve photoresponse are the use of beryllium rather than zinc implants (the lighter beryllium ion produces only about 3% of the lattice damage produced by zinc), and implantation through a silicon dioxide layer to shift the peak of the implanted distribution to the surface, eliminating the region near the surface in which the built-in field opposes the flow of minority carriers to the junction.

A comparison of our results with published results suggests that, if we can satisfactorily resolve the surface region photoresponse problem, we will be able to fabricate a high efficiency gallium arsenide solar cells by beryllium implantation.

2. EXPERIMENTAL INVESTIGATIONS

2.1 Characteristics of Zn^+ Implanted Diodes and Solar Cells

The detailed experimental results of zinc ion implantation and annealing experiments have been reported in Quarterly Report No. 2. It was shown that for Zn^+ implants of 600 to 800 keV and dose level between 1×10^{15} to 5×10^{15} cm^{-2} the resultant sheet resistances and junction depths on a N type substrate with $N_D \simeq 2 \times 10^{17}$ cm^{-3} are close to the optimum cell design parameters as computed from solar cell junction theory. During this quarter, we fabricated solar cells and mesa diodes, employing 600 and 800 keV Zn^+ implantations with doses of 2×10^{15}, and 1×10^{16} cm^{-2} into N type 0.009 Ω cm ($N_D \simeq 2 \times 10^{17}$ cm^{-3}) material. Post-implantation annealing was done at 700 °C for 30 minutes with 0.3 micron sputtered silicon oxide covering the implanted surface. Silver-based metal contacts were then evaporated on front implanted and back substrate surface, (see Section 2.4 for procedure). A small portion of the experimental sample is used to form mesa diodes with typical area $\simeq 10^{-3}$ cm^2, while the larger portion of the sample has a tapered finger grid contact evaporated onto the front surface for illuminated measurements.

Table 1 summarizes the measurements on the mesa diodes. The implanted layer sheet resistance and junction depth measurements are reproducible from the previous experiments. From the C-V measurement it is obvious that the P^+N junction is nearly abrupt, and the calculated background concentration from the measured Co/A of 90 nf/cm^2 is 1.8×10^{17} cm^{-3}. The forward I-V measurements indicate that the junction current is controlled by recombination in the space charge region for $V_f \lesssim 0.9$ V, as is true of GaAs diodes formed by zinc diffusion.

The illuminated measurements are summarized in Table 2. The low short-circuit density J_{sc} is obviously a disappointing experimental fact. In contrast to the theoretical value of 35 mA/cm^2, the highest observed value is only 5.63 mA/cm^2. The low values of open-circuit voltage result both from the low short-circuit current density and from junction nonuniformity, as further discussed below.

Figure 1 shows the spectral response of the short circuit current for a 600 keV Zn^+ implanted solar cell. The blue end of the response starts at $\lambda = 0.5$ micron and suggests that the surface region down to a depth of at least $\alpha^{-1} = 0.24$ micron* has such a high recombination rate that the photogenerated

*At $\lambda = 0.5$ micron the absorption coefficient α in GaAs is 4.2×10^4 cm^{-1}.

Table 1. Characteristics of Zn^+ Implanted P^+N GaAs Mesa Diodes.

Impl. Energy (keV)	Dose (cm^{-2})	$\bar{\rho}_s$ * ($\Omega/\square$)	x_j (μm)	Co/A (nf/cm^2)	n ($C \sim V^{-n}$)	A for $V_f < 0.9$ V $\left(\ln I_f \sim \frac{q}{AkT} V_f\right)$
600	2×10^{15}	170	0.38	#1 80.7	0.42	2.5
				#2 66.4	0.39	2.33
				#3 79.2	0.43	2.42
600	5×10^{15}	85.8	0.45	#1 86.8	0.46	2.33
				#2 93.2	0.47	2.33
600	1×10^{16}	49.7	0.50	--	--	--
800	2×10^{15}	108	0.50	#1 81.4	0.43	2.33
				#2 87.7	0.45	2.50
800	5×10^{15}	68	0.55	#1 89	0.47	2.17
				#2 91	0.49	2.33
800	1×10^{16}	52.4	0.65	#1 90.5	0.48	2.33

*Anneal at 700 °C for 30 minutes.

Table 2. Characteristics of Zn^+ Implanted P^+N GaAs Solar Cells.

Sample	Impl. Energy, Dose (keV, cm^{-2})	Anne. Temp., Time ($^{\circ}C$, min.)	Area (cm^2)	J_{sc} (mA/cm^2)	Voc (Volt)	F.F.*
1A	800, 2×10^{15}	700, 30	1.1	5.63	.605	.63
1B	800, 2×10^{15}	700, 30	.95	4.70	.578	.62
2A	600, 5×10^{15}	700, 30	.97	4.12	.580	.56
3A	800, 2×10^{15}	650, 180	.63	2.14	.550	.65
3B	800, 2×10^{15}	650, 180	.245	2.45	.545	.50
4A	800, 5×10^{15}	650, 180	.475	3.05	.476	.46
5A	800, 2×10^{15}	800, 30	1.94	5.0	.52	.39
5B	800, 2×10^{15}	800, 30	1.46	4.3	.49	.42
6A	600, 5×10^{15}	800, 30	1.71	3.67	.605	.55

*F.F. = Form Factor = $\frac{I_{mp} V_{mp}}{I_{sc} V_{oc}}$

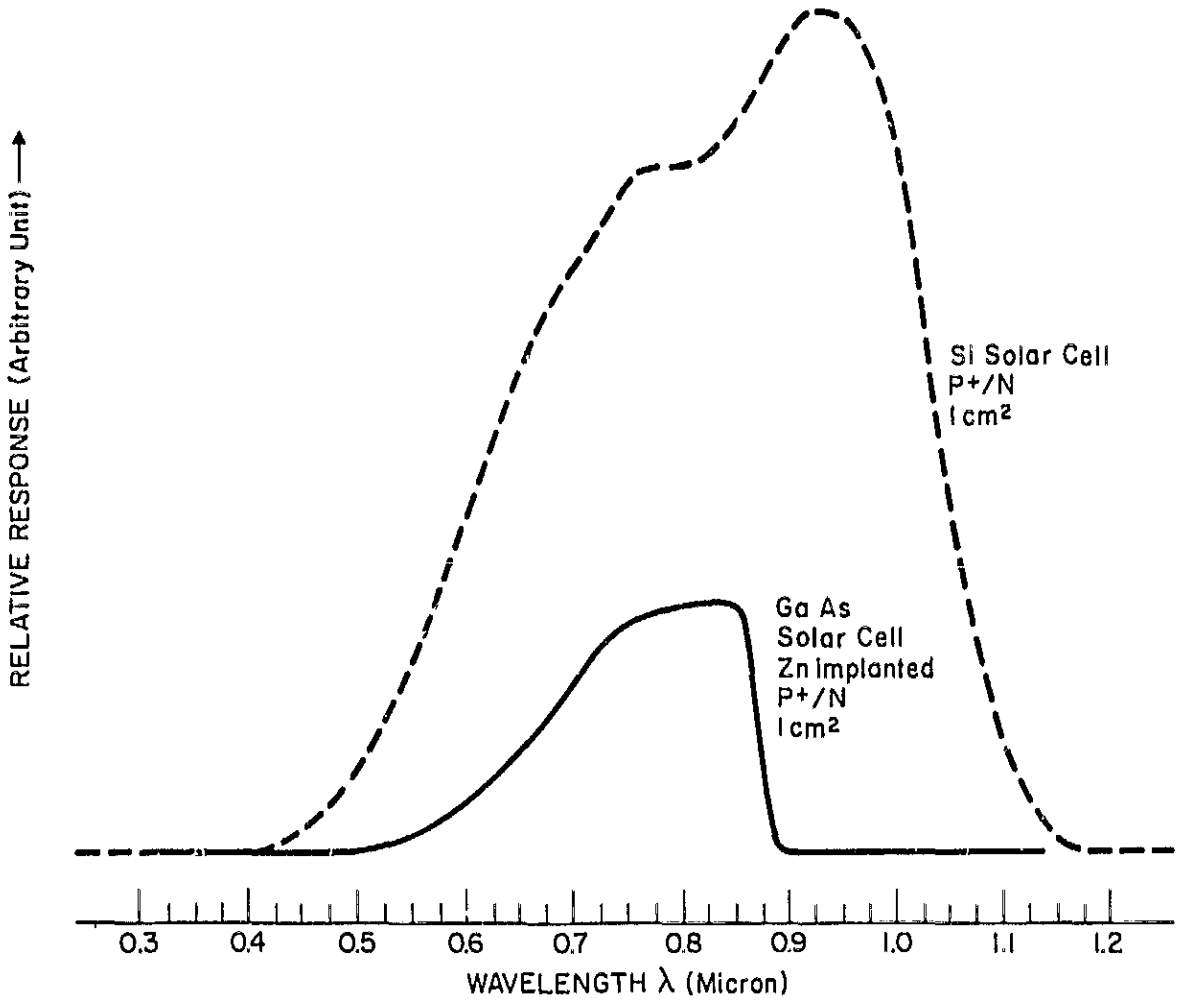

Figure 1. Relative Spectral Response of Zn^+ Implanted GaAs Solar Cell

1-6413

carriers will recombine before reaching the junction and so do not contribute to the short-circuit current. A similar "dead layer" has been observed on unidiffused samples by Wittry and Kyser[1], and on diffused samples by Kalibjian and Mayeda.[2] In our samples, we believe that this surface dead layer results from the presence of a high density of recombination centers at or near the surface, produced either in the polishing or implantation steps and not removed by subsequent annealing. The effect of these centers is enhanced by the fact that the peak of the implanted acceptor distribution occurs some distance into the sample, so that the built-in field in the region between the surface and the peak of the distribution causes photogenerated minority carriers to drift towards the surface rather than towards the junction. It is significant that the thickness of the dead layer, as deduced from the spectral response, is approximately equal to the depth of the peak of the implanted acceptor distribution.

In order to improve short-circuit current density, it is apparent that we should adjust the acceptor profile so that the peak concentration occurs at the surface; also, we should attempt to discover the sources of processing-induced defects in the surface region and adjust the fabrication procedure to minimize them. A more nearly optimum profile can be obtained by implanting through a silicon dioxide layer of properly chosen thickness; this will also protect the surface against contamination and mechanical damage during implantation. Radiation damage during implantation can be minimized by using the lightest dopant ion available. Hunsperger et al.[3] have reported that beryllium is an effective acceptor dopant in gallium arsenide. The small mass of the beryllium ion allows the use of much lower ion energies to obtain the same penetration, and a larger fraction of the ion energy is dissipated in electronic excitation rather than in the production of displacement damage. This is the reason behind our decision to investigate beryllium implants.

2.2 Characteristics of Be^+ Implanted Diodes and Solar Cells

Beryllium ions were generated from solid beryllium fluoride in an arc-discharge ion source. Analyzed beam currents of several microamperes were easily achieved. Values of projected range and standard deviation of

---

(1) D.B. Wittry, D.F. Kyser: "Surface Recombination Velocities and Diffusion Lengths in GaAs", Proc. of the Int. Conf. on the Phys. of Semicond. Kyoto, p. 312, (1966).

(2) R. Kalibjian, K. Mayeda: "Characteristics of GaAs Photovoltaic Diodes at Low Irradiance", Solid-State Electronics 12, 823 (1969).

(3) R.G. Hunsperger et al: "Mg and Be Ion Implanted GaAs", Jour. of Appl. Phys. 43, 1318 (1972).

projected range were calculated from LSS theory. The calculated acceptor concentration profiles for a total dose of 10^{15} Be^+/cm^2 and ion energies of 40, 70 and 100 keV are shown in Figure 2. The profiles for beryllium at 70 and 100 keV are closely similar to those calculated for zinc ions of 600 and 800 keV.

Table 3 presents the results of measurements on the beryllium-implanted samples. The samples were annealed at 700 °C for 20 minutes in forming gas after implantation and deposition of a protective silicon dioxide coating. A comparison with the zinc-implanted samples (Table I) shows that the sheet resistance and junction depth for beryllium implants of 1×10^{15} cm^{-2} is equivalent to those obtained with zinc implants of 2×10^{15} cm^{-2} and eight times higher energy. It therefore appears that nearly 100% activation of the implanted acceptors can be achieved by annealing beryllium-implanted samples to 700 °C, while zinc-implanted samples require 800 °C. Other parameters are similar to the zinc-implant data.

The illuminated solar cell output characteristics are summarized in Table 4. The short circuit densitities do not show appreciable improvement over Zn^+ implanted solar cells. Spectral response data of Figure 3 suggests that a similar "dead layer" exists in the Be^+ implanted surface region.

A single 2×2 cm^2 solar cell, beryllium-implanted at 100 keV, was divided into 4 sections approximately 1×1 cm in size. The four sections showed similar values of short-circuit current density, but there was a large variation in other parameters, as shown in Table IV and Figure 4. The dark I-V characteristic for sample #4 shows values of forward current at low voltages which are as low as the best gallium arsenide cell values reported in the literature.[4] The other segments showed higher currents. Etching the edges of these samples did not change the I-V characteristic appreciably.

The two worst sections (Group A) were the sections on which the contact bar was deposited (Figure 5). Angle sections of the contact bar region were made to check for penetration of the junction by the metallization, but no evidence of this was found.

From these samples, we concluded that the high-recombination layer at the surface which was responsible for the low values of short-circuit current could in localized regions extend to the depth of the junction. Such non-uniform damage would most probably result from mechanical damage prior to implantation. We therefore re-examined our surface preparation techniques to determine

---

[4] Kagan, Landsman, Lyubashevskaya, and Kholev: "High-Efficiency Gallium Arsenide Solar Cells and Possible Improvements", Geliotekhnika 3, 10 (1967).

Table 3. Characteristics of Be^+ Implanted P^+N GaAs Mesa Diodes.

Impl. Energy (keV)	Dose (cm^{-2})	$\bar{\rho}_s$* ($\Omega/\square$)	x_j (μm)	Co/A (nf/cm^2)	($C \cdot V^{-n}$)	A for $V_f < .9$ V $\left(\ln I_f \sim \frac{q}{AkT} V_f\right)$
100	10^{15}	110	.52	#1 80	.45	2.16
				#2 82.2	.45	2.33
70	10^{15}	158	.48	#1 83.2	.45	2.16
40	10^{15}	815	-	#1 57.4	.304	2.16

*Anneal at 700 °C for 20 minutes.

Table 4. Characteristics of Be^{+} Implanted $P^{+}N$ GaAs Solar Cells.

Sample	Impl. Energy, Dose (keV, cm^{-2})	Anne. Temp., Time ($^{\circ}C$, min.)	Area (cm^2)	J_{sc} (mA/cm^2)	V_{oc} (Volt)	F.F.
1A	100, 10^{15}	700, 20	.91	4.84	.538	.48
1B	100, 10^{15}	700, 20	.93	5.0	.660	.58
1C	100, 10^{15}	700, 20	.90	5.05	.796	.75
1D	100, 10^{15}	700, 20	.93	5.14	.810	.79
2A	70, 10^{15}	700, 20	.645	6.47	.672	.59
3A	40, 10^{15}	700, 20	.77	6.37	.530	.61

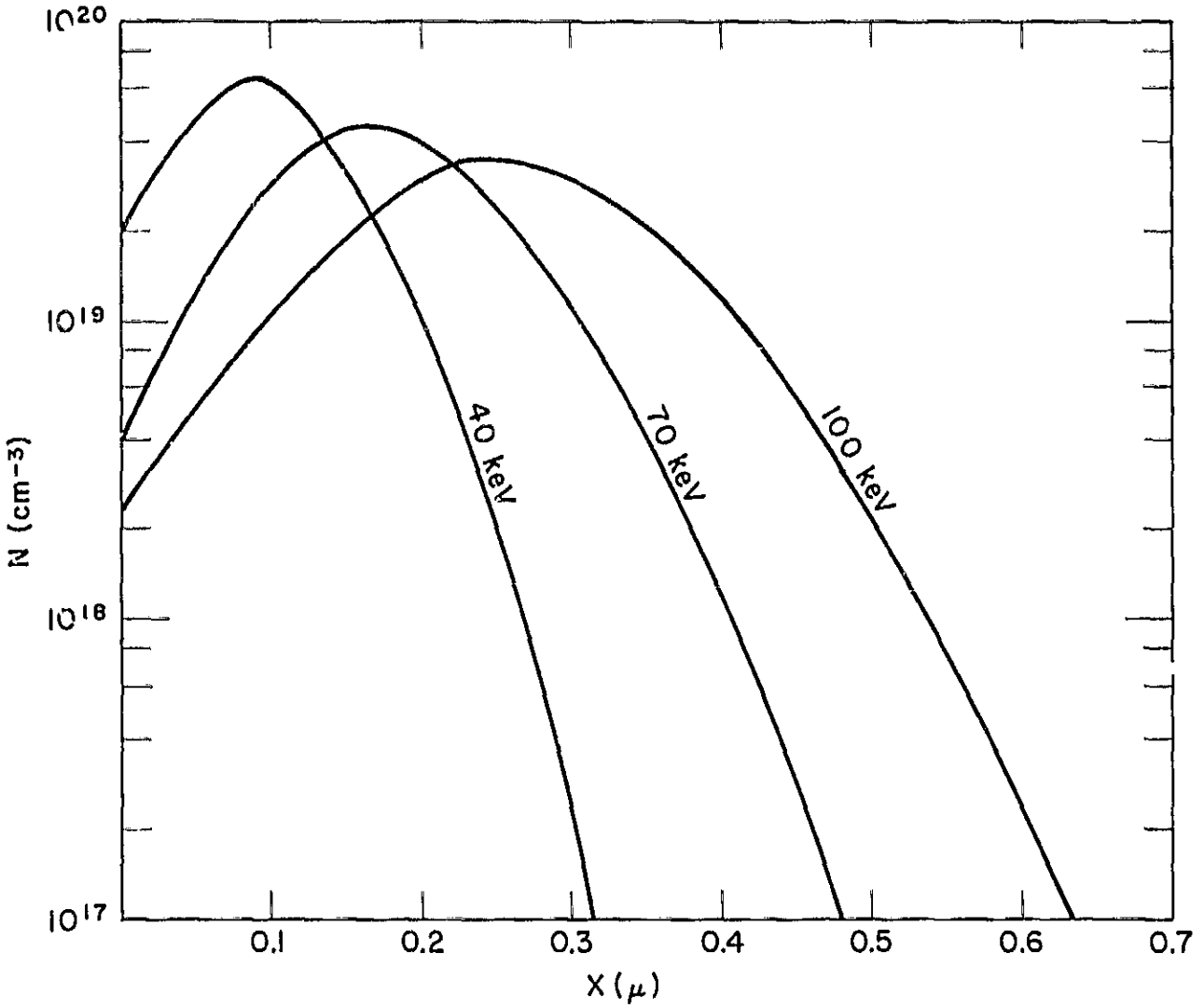

Figure 2. Calculated Beryllium Ion Distribution in GaAs For Energies of 40, 70, 100 keV and Dose of 10^{15} cm^{-2}.

1-6414

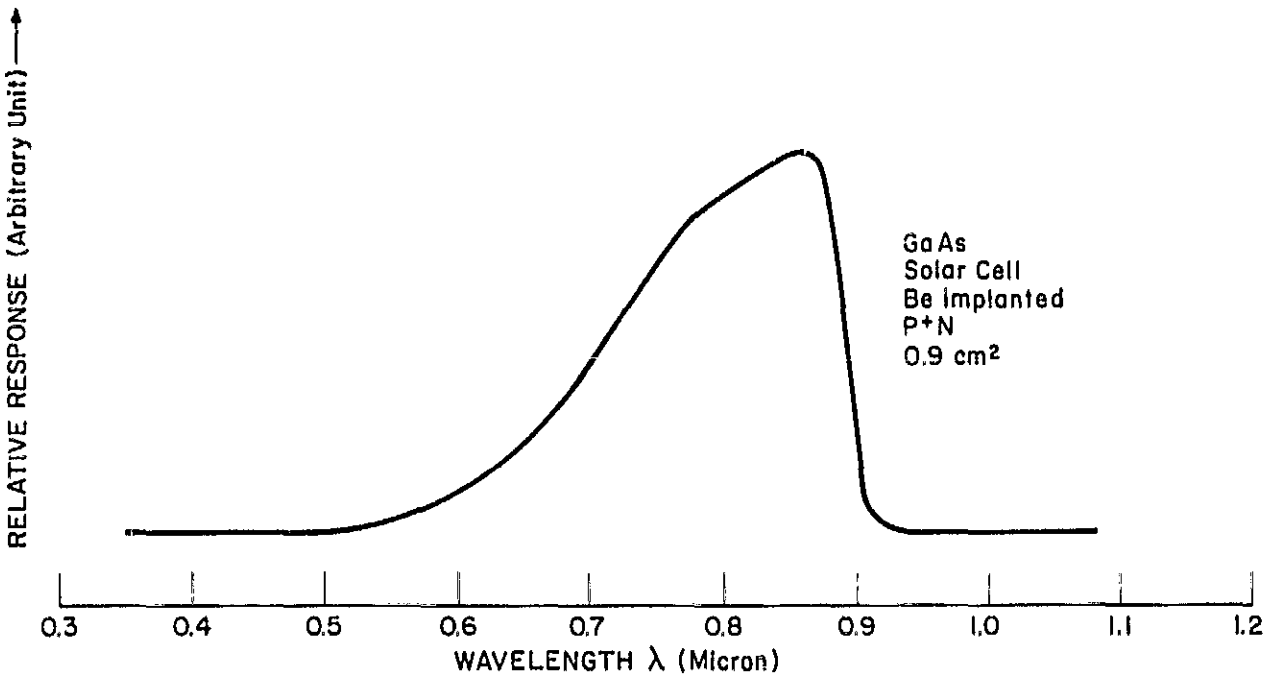

Figure 3. Relative Spectral Response of Be^+ Implanted GaAs Solar Cell.

1-6415

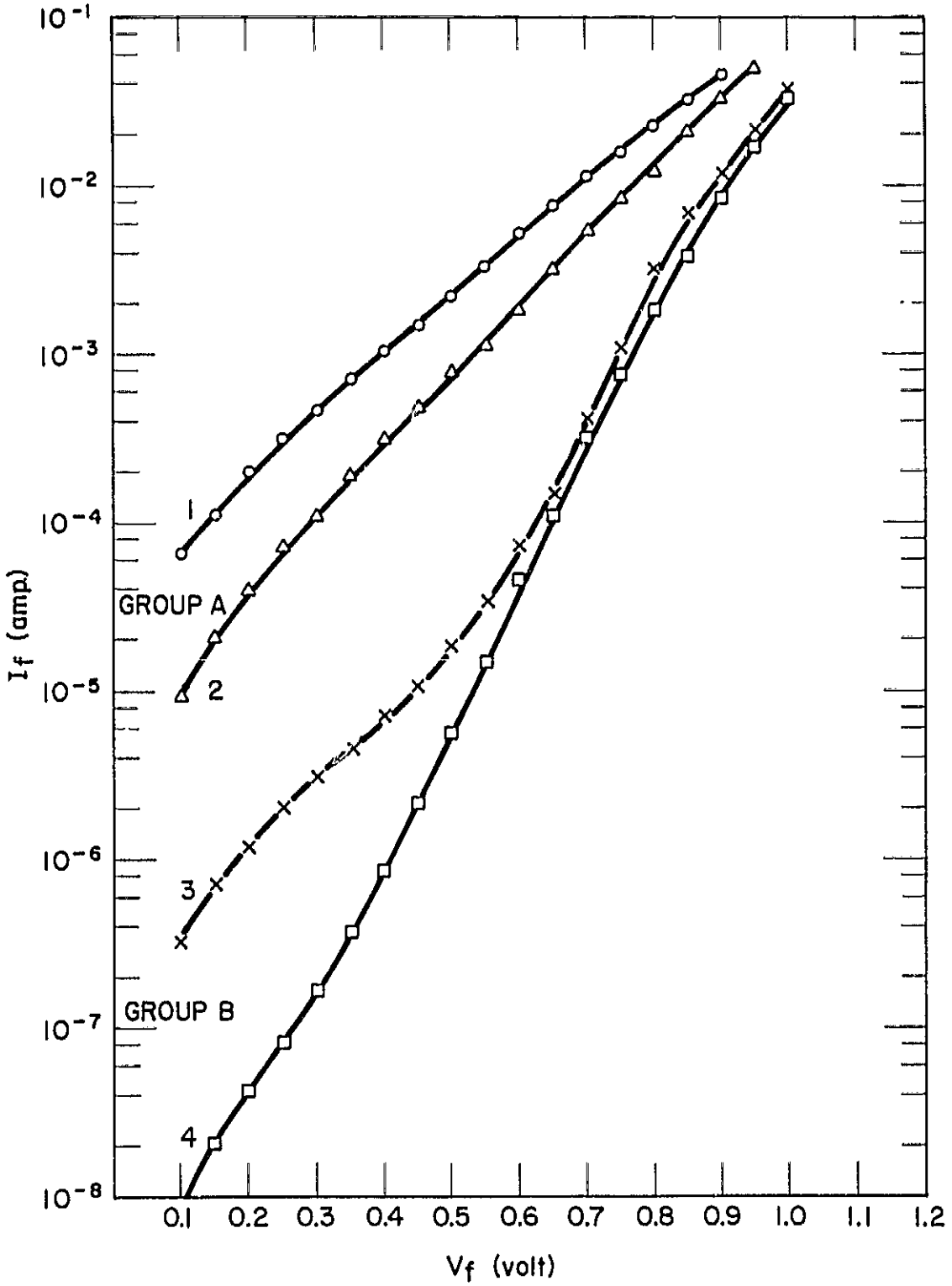

Figure 4. Dark Forward I-V Characteristics of a Be^+ Implanted (100 keV, 10^{15} cm^{-2}) P^+N Solar Cell (4 cm^2) Scribed into Four Small Samples

1-6416

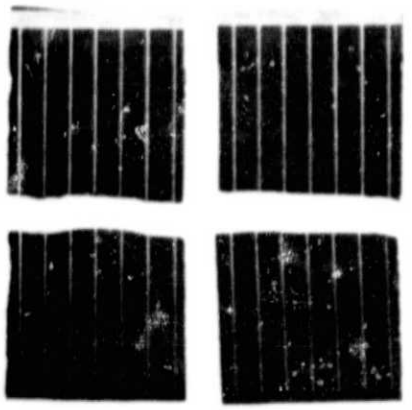

Figure 5. A Be^{+} Implanted (100 keV, 10^{15} cm^{-2}) $P^{+}N$ Solar Cell (4 cm^{2}) Scribed Into Four Small Samples. Celi #1 and #2 (Group A) Have Larger Contact Area Than Cell #3 and #4 (Group B).

if all polishing damage was being removed prior to implantation. This investigation is described in the following section of this report.

Although the beryllium-implanted cells produced during this report period were no better than the zinc-implanted cells, we believe that beryllium implantation will prove better than zinc implantation. The lower annealing temperature required for full activation of the beryllium implants supports the calculations of lower defect introduction rate. During the remainder of the contract, we intend to fabricate samples by implanting beryllium through a thin mask of sputtered silicon dioxide.

2.3 Improvement of Surface Preparation

The two-step polishing procedure discussed in the Second Quarterly Report was more extensively investigated during the past month. Samples previously polished and processed through to a final solar cell configuration were given a light etch in a 5% solution of bromine and methanol to determine the extent of work damage from previous processing steps. The results showed large numbers of scratches across the entire cell surface (Figure 6) which by their nature in shape and pattern strongly suggested they originated at initial polishing. Further investigation revealed that the first polishing step operation (chem-mechanical polishing with 2% sodium hypochlorite solution) in some instances, created deep scratches not apparent to the naked eye. It was further determined that the second polishing step (chemical etch in a 5% solution of bromine in methanol) did not bring out these underlying scratches because the etchant was not utilized for an adequate length of time.

Due to the uncertainty and close operate control required of this procedure, a modification was made. The following is the revised procedure:

(1) Etch A and B faces in a solution of 1% by volume of bromine in methanol for 1 minute.

(2) Mount A face down on glass slat and lap B face to a uniform finish with 5 micron diamond grit.

(3) Chem-mechanical polish B face on Pellon cloth by hand using 1% by volume bromine in methanol. Complete to high polish finish.

(4) Etch in 1% by volume bromine in methanol for 1 minute and rinse thoroughly in methanol.

(5) Etch in 1 H_2SO_4 : 1 H_2O_2 : 1 H_2O solution for 30 seconds and rinse thoroughly in deionized water.

(6) Dismount slice. Clean and vapor degrease in trichloroethylene.

Figure 6. Finished Solar Cell with Surface Scratches Resulting From Mechanical Polish After Delineation From Br/Methanol Etch.

Samples prepared by the revised procedure showed no evidence of scratches on further etching.

2.4 Improved Contacting Procedure

As previously discussed in Monthly Progress Report No. 6, considerable efforts have been devoted to improving the InAg contacting procedure. Initially, much difficulty was encountered in forming reproducibly adherent alloy contacts on both surfaces of the implanted layer. The contact adherence was greatly improved by etching in 1 H_2SO_4 : 1 H_2O_2 : 100 H_2O for 30 seconds just prior to contact evaporation. The amount of material removed by the etch is negligible. Contact resistance between the metal and the semiconductor has been further reduced by adding to the In metal, 10% Zn for the P type implanted layer and 10% Sn for the N type substrate during sequential evaporation.

The contacts produced by the revised procedure not only withstand the usual tape and abrasion tests, but after firing for 5 minutes at 560 °C in hydrogen, will withstand vigorous abrasion with metal tweezers without peeling. The contacts therefore appear to be comparable in adhesion to the TiAg contacts normally used on silicon solar cells. No contact failures have occurred during handling, including ultrasonic bonding of electrical leads, and the measured I-V characteristics show no evidence of appreciable series resistance. We therefore conclude that this procedure is adequate for the purposes of this contract.

3. CONCLUSIONS AND FUTURE PLANS

It is obvious that the main task for the remainder of the program will be the improvement of cell short-circuit current density. A surface "dead layer" is responsible for the low values of short-circuit current observed in devices fabricated to date; in the best devices the junction quality and base region lifetime appear to be as good or better than the best values reported in the literature. Both the mechanical preparation of the surface prior to implantation and the implantation technique itself appear to be at fault. The improved surface preparation process described in Section 2.3 appears to yield damage-free surfaces, to the extent that this can be determined by etching with structure-sensitive etchants. The implantation process needs further improvement. The substitution of beryllium for zinc is a step in the right direction, but additional work must be done to optimize the dopant profile and post-implantation annealing schedule. Although the implantation and annealing schedules used to date have produced surface layers with the desired junction depth and sheet resistance, an insufficient number of measurements of cell spectral response have been made to optimize the surface layer photoresponse.

During the next quarter, we will use spectral response measurements to optimize the implantation and annealing processes. Implantation will be done through an oxide layer to place the peak of the implanted ion distribution at the gallium arsenide surface. Annealing at higher temperature (to 850 °C) will be evaluated.

In view of the limited time remaining in the program, it will be necessary to curtail certain items of work originally planned. An experimental investigation of N^+P cells does not appear to be worthwhile, since the only cell parameter which appears to be favored by the N^+P structure, according to the calculations presented in the first quarterly report, is the cell series resistance (due to the lower sheet resistance of the N^+ layer). Since we have demonstrated that P^+ layers can be produced with sheet resistances of about 150 ohms/square, which result in a contribution to cell series resistance of about 0.1 ohm for a 2 x 2 cm cell with our 14-finger front contact, we are not limited by surface layer sheet resistance. A significant disadvantage of the N^+P structure is that it requires higher lifetime in the surface region than the P^+N structure, because the built-in field produced by the doping gradient in the surface layer has less effect on promoting the drift of holes to the junction, for an N^+ layer, than it does on electrons in a P^+ layer. Since surface region recombination appears to be the major factor limiting cell performance, the N^+P structure appears to be unfavorable.